Novel human adenosine receptor antagonists based on the 7-amino-thiazolo[5,4-d]pyrimidine scaffold. Structural investigations at the 2-, 5- and 7- positions to enhance affinity and tune selectivity.

Flavia Varano [a,*], Daniela Catarzi [a], Matteo Falsini [a], Diego Dal Ben [b], Michela Buccioni [b], Gabriella Marucci [b], Rosaria Volpini [b], Vittoria Colotta [a]

[a] Dipartimento di Neuroscienze, Psicologia, Area del Farmaco e Salute del Bambino, Sezione di Farmaceutica e Nutraceutica, Università degli Studi di Firenze, via Ugo Schiff, 6, 50019, Sesto Fiorentino, Italy. [b] Scuola di Scienze del Farmaco e dei Prodotti della Salute, Università degli Studi di Camerino, Via S. Agostino 1, 62032 Camerino, MC, Italy

Corrisponding author:

*Tel: +39 055 4573732. Fax: +39 055 4573780. E-mail: flavia.varano@unifi.it.

Abstract

This paper describes the synthesis of novel 7-amino-thiazolo[5,4-d]pyrimidines bearing different substituents at positions 2 , 5 and 7 of the thiazolopyrimidine scaffold. The synthesized compounds **2-27** were evaluated in radioligand binding (A_1, A_{2A} and A_3) and adenylyl cyclase activity (A_{2B} and A_{2A}) assays, in order to evaluate their affinity and potency at human adenosine receptor subtypes. The current study allowed us to support that affinity and selectivity of 7-amino-thiazolo[5,4-d]pyrimidine derivatives towards the adenosine receptor subtypes can be modulated by the nature of the groups attached at positions 2, 5 and 7 of the bicyclic scaffold. To rationalize the hypothetical binding mode of the newly synthesized compounds, we also performed docking calculations in human A_{2A}, A_1 and A_3 structures.

KEYWORDS. G protein coupled receptors; adenosine receptors; adenosine receptor antagonists; thiazolopyrimidine derivatives; bicyclic heteroaromatic system.

Adenosine receptors (ARs) are members of the G protein-coupled receptors superfamily and comprise four subtypes designated A_1, A_{2A}, A_{2B}, and A_3 [1]. A_{2A} and A_{2B} ARs are mainly coupled to G_s proteins while A_1 and A_3 ARs are generally coupled to G_i proteins, thus leading to an enhancement or decrease of intracellular cAMP levels, respectively. Additionally, the various AR subtypes may interact with other classes of G proteins leading to activation of various second messenger pathways, such as phospholipase C, mitogen activated protein kinase, potassium and calcium channels, arachidonic acid pathways, and phospholipase D [1].

It is well known that ARs, due to their different organ and tissue distribution in the human body, are implicated in numerous and important physiopathological processes [2, 3]. In particular, the blockade of ARs was studied for the treatment of heart and renal failure [4-6], cognition disorders [7] (A_1 AR), neurodegenerative diseases [8-9], dermal fibrosis [10-12], retinal dysfunctions [13], cancer [14-17], and pain [18] (A_{2A} AR), inflammatory lung diseases such as asthma [19] (A_{2B} AR), airway contraction, glaucoma and cancer [20-22] (A_3 AR).

In continuation of our studies directed towards the identification of new AR antagonists [23-28], in a recent paper we disclosed the 5-methyl-2-phenylthiazolo[5,4-d]pyrimidin-7-one **1** [29] which proved to be a potent and selective human (h) A_3 AR antagonist, being inactive at the other AR subtypes (Fig. 1). To further explore the structure affinity relationships (SARs) in this class of AR antagonists, we here describe the synthesis of the 7-amino-5-methyl-2-phenylthiazolo[5,4-d]pyrimidine **2** which is the 7-amino analogue of **1** (Fig. 1). The replacement of the 7-oxo function with a 7-amino group is a structural modification that in other classes of bicyclic AR antagonists significantly modified AR affinity and selectivity [30, 31]. Moreover, we recently disclosed the thiazolo[5,4-d]pyrimidine-5,7-diamino series which shows an extraordinary high affinity for the hA_{2A} AR subtype [18, 32-33]. Anticipating the results, it emerged that the 7-amino derivative **2** showed good affinity for the hA_{2A} and for the hA_1 AR and a low binding activity at the hA_3 subtype. This result prompted us to further investigate the 7-aminothiazolo[5,4-d]pyrimidine series

by combining a phenyl or a furan-2-yl ring at position 2 with an aryl or heteroaryl group at position 5 (compounds **3-20**, Fig. 1). Furthermore, we also investigated the effect on AR affinity and selectivity of introduction of different acyl residues on the 7-amino moiety (compounds **21-27**, Fig. 1). Acyl residues on the 7-amino group were chosen since they increased hA_3 AR affinity and selectivity in many classes of AR antagonists of similar size and shape [20, 22, 28]. All the newly synthesized compounds (**2-27**) were tested in binding assays to evaluate their affinity at cloned hA_1, hA_{2A} and hA_3 ARs, stably expressed in Chinese Hamster Ovary (CHO) cells. Compounds were also tested at hA_{2A} and hA_{2B} ARs by measuring their inhibitory effects on NECA-stimulated cAMP levels in CHO cells.

Figure 1.

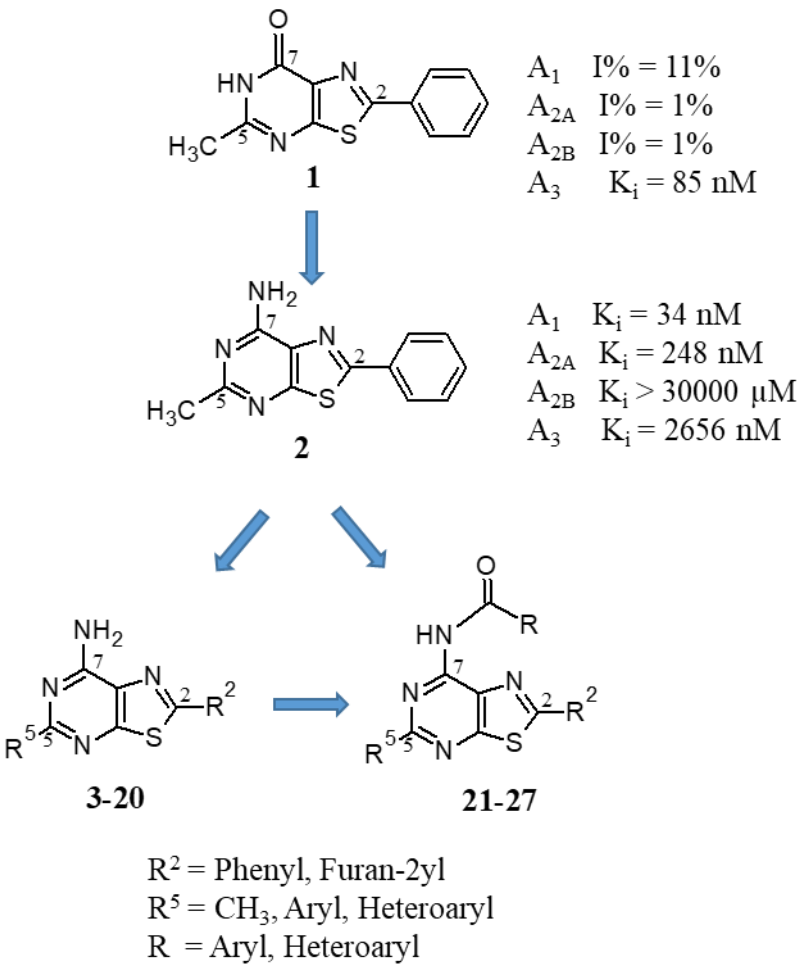

Along with the pharmacological evaluation, docking studies at hA_1, hA_{2A} and hA_3 AR structures were performed to rationalize the observed affinity data.

Compounds **2-27** were synthesized according to the procedures depicted in Schemes 1-3. The 7-amino-2-phenyl-5-methyl derivative **2** was obtained (95% yield) starting from its 7-oxo analog **1** synthesized as previously reported by us (Scheme 1) [29]. The 7-oxo compound **1** was treated with $POCl_3$ to yield the 7-chloro derivative **28** [29], which upon reaction with aqueous ammonia solution furnished the desired 7-amino derivative **2**.

Scheme 1

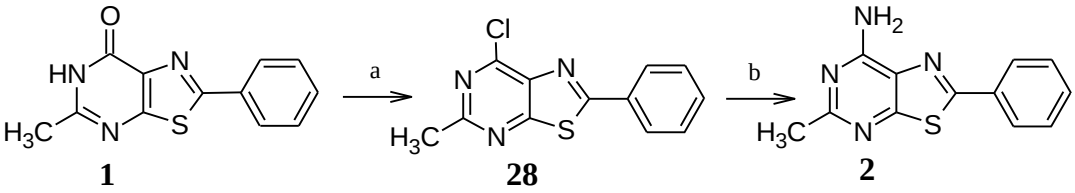

Reagents and conditions: (a) $POCl_3$, dimethylaniline, reflux, 3h; (b) NH_3(g), EtOH, sealed tube, 130 °C, overnight, 95% yield.

Compounds 2-phenyl- **3-11** and 2-(furan-2-yl)- substituted **12-20** were synthesized reacting the corresponding 5-chloro derivatives **29** [33] and **30** [18] and the suitable boronic acids under Suzuki conditions (Scheme 2).

Finally, the 7-amino derivatives **2**, **3** and **12** by reaction with the proper acyl chlorides yielded the desired 7-acylamino substituted **21-27** (Scheme 3).

Schema 2.

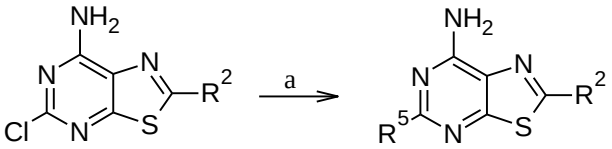

29 R^2 = phenyl
30 R^2 = furan-2yl

3-11 R^2 = phenyl
12-20 R^2 = furan-2yl

	R^5
3, 12	C_6H_5
4, 13	C_6H_4-3-CH_2OH
5, 14	C_6H_4-4-CH_2OH
6, 15	C_6H_4-4-OCH_3
7, 16	C_6H_4-3-OCH_3
8, 17	C_6H_4-3-CN
9, 18	C_6H_4-3-OH
10, 19	furan-2-yl
11, 20	5-methylfuran-2-yl

Reagents and conditions: (a) $R^5B(OH)_2$, tetrakis, Na_2CO_3, DME/H_2O, microwave irradiation, 160 °C 30 min (**3**-**4**, **6**-**7**, **12**-**13**, **17**-**18**), 35-68% yield, or reflux 4h (**5**, **8**-**11**, **14**-**16**, **19**-**20**), 30-72% yield.

Scheme 3

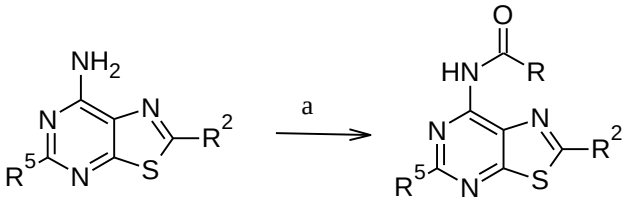

2 $R^2 = C_6H_5$ $R^5 = CH_3$

3 $R^2 = C_6H_5$ $R^5 = C_6H_5$

12 R^2 = furan-2yl $R^5 = C_6H_5$

21-23 $R^2 = C_6H_5$ $R^5 = CH_3$

24-25 $R^2 = C_6H_5$ $R^5 = C_6H_5$

26-27 R^2 = furan-2yl $R^5 = C_6H_5$

	R
21, 24, 26	C_6H_5
22	C_6H_4-4Cl
23	C_6H_4-4OCH_3
25, 27	furan-2-yl

Reagents and conditions: (a) RCOCl, Pyridine dry, CH_2Cl_2, reflux, 3-4 days, 20-55% yield.

The new thiazolo[5,4-d]pyrimidine derivatives **2-20** and **21-27** were evaluated for their affinity to hA_1, hA_{2A} and hA_3 ARs, stably transfected in CHO cells, and were also tested at the hA_{2B} AR subtype by measuring their inhibitory effects on 5'-(N-ethyl-carboxamido)adenosine (NECA)-stimulated cAMP levels in hA_{2B} CHO cells. The selected derivatives **9**, **10**, **18** and **19**, showing high affinity for the hA_{2A} AR, were investigated to determine their antagonistic potency by measuring their effects on cAMP production in CHO cells, stably expressing hA_{2A} ARs.

The results of binding experiments carried out on the new thiazolo[5,4-d]pyrimidine derivatives **2-20** and **21-27** are displayed in Tables 1 and 3, respectively. Concerning the hA_{2B} AR, compounds **2-20** and **21-27** were inactive in inhibiting the NECA-stimulated cAMP levels in hA_{2B} CHO cells (IC_{50}> 30000 nM, data not shown).

In general, results of some interest have been obtained for the 7-amino derivatives **2-20** (Table 1). In fact, all the reported compounds bind the hA_1, hA_{2A} and hA_3 ARs with good affinities. More specifically, compounds **9**, **12**, **17**, **18**, **19**, **20** showed nanomolar affinity toward the hA_{2A} AR subtype and a good degree of selectivity for this receptor. Worthy of note is the presence of a furan-2-yl at both 2 and 5 positions producing the best combination of hA_{2A} AR affinity and selectivity (compound **19**). Compounds **10**, **13**, **14**, **15**, **16**, were able to bind both the hA_{2A} and hA_3 ARs showing comparable K_i values falling in the nanomolar range. Finally, two derivatives (compounds **4** and **5**) having nanomolar affinity and good selectivity for the hA_3 AR subtype were identified.

Analyzing the binding data, we observe that the replacement of the 5-methyl group of **2** by a phenyl residue (compound **3**) led to a noteworthy increase in hA_{2A} and hA_3 AR affinity while the hA_1 AR binding activity decreases.

Table 1. Binding affinity of compounds **2-20** at hA_1, hA_{2A} and hA_3 ARs.[a]

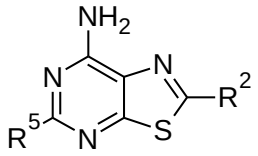

2-20

	R^2	R^5	binding experiments K_i (nM)			A_{2A} AR selectivity	
			hA_1[b]	hA_{2A}[c]	hA_3[d]	A_1/A_{2A}	A_3/A_{2A}
2	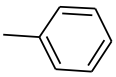	CH_3	34 ± 1	248 ± 33	2656 ± 235	0.14	10.7
3		C_6H_5	148 ± 16	19 ± 6.2	84 ± 13	7.8	4.4
4		C_6H_4-3-CH_2OH	32 ± 9	53 ± 13	3.7 ± 1.2	0.6	0.07
5		C_6H_4-4-CH_2OH	82 ± 17	82 ± 19	8.2 ± 0.5	1	0.1
6		C_6H_4-4-OCH_3	224.6 ± 61.3	115.3 ± 5.1	46.7 ± 12	1.9	0.4
7		C_6H_4-3-OCH_3	175.9 ± 34.7	109.8 ± 0.35	35.6 ± 9.2	1.6	0.3
8		C_6H_4-3-CN	594 ± 124	33.6 ± 8.9	247 ± 74	17.7	7.3
9		C_6H_4-3-OH	58.5 ± 6.1	5 ± 1.5	190 ± 16.7	11.7	38
10		furan-2-yl	67 ± 6.8	1.7 ± 0.2	2.8 ± 0.4	39.4	1.6
11		5-CH_3-furan-2-yl	28.9 ± 6.6	22.4 ± 4.03	24.9 ± 3.4	1.3	1.1
12	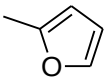	C_6H_5	33 ± 2	3 ± 0.04	15 ± 2.9	11	5
13		C_6H_4-3-CH_2OH	28 ± 5.5	2.1 ± 0.3	0.9 ± 0.1	13	0.4
14		C_6H_4-4-CH_2OH	77.7 ± 14.5	7.7 ± 0.45	3.58± 0.41	10.1	0.5
15		C_6H_4-4-OCH_3	47.7 ± 3.4	11.2 ± 0.83	4.66 ± 1.2	4.2	0.4
16		C_6H_4-3-OCH_3	62.3 ± 5.1	1.9 ± 0.33	4.90 ± 0.19	32.8	2.6
17		C_6H_4-3-CN	102.7 ± 6.8	7.7 ± 1.4	61.5 ±14.1	13.3	8.0
18		C_6H_4-3-OH	51.0 ± 1.6	1.64 ± 0.35	15.73 ± 3.5	31.1	9.6
19		furan-2-yl	69 ± 15	3.4 ± 0.9	99 ± 15	20.3	29.1
20		5-CH_3-furan-2-yl	45.9 ± 4.4	2.36 ± 0.4	13.76 ± 1.7	19.4	5.8

[a]Data (n = 3−5) are expressed as means ± standard errors. [b]Displacement of specific [^{3}H]-CCPA binding at hA_1 AR expressed in CHO cells. [c]Displacement of specific [^{3}H]-NECA binding at hA_{2A} AR expressed in CHO cells. [d]Displacement of specific [^{3}H]-HEMADO binding at hA_3 AR expressed in CHO cells.

Introduction of substituents on the appended 5-phenyl ring (compounds **4-9**) results in different effects depending on the receptor subtype. In fact, only the presence of a meta hydroxy substituent (compound **9**) increases the affinity leading to a potent and selective hA_{2A} AR antagonist (K_i = 5 nM). For hA_3 AR anchoring the best substituent was the hydroxymethyl one both in the meta or para positions (compounds **4** and **5**). Finally, binding at the hA_1 AR was only slightly enhanced by a hydroxy substituent both directly attached (compound **9**) or spaced by a methylene group (compound **4-5**).

Replacing the 5-phenyl moiety of derivative **3** with a furan-2-yl ring resulted in compound **10** which showed enhanced affinity towards all three receptors, with the greatest increase observed for the hA_{2A} and hA_3 AR subtypes, (K_i = 1.7 nM and K_i = 2.8 nM, respectively).

Subsequently, we synthesized compounds **12-20** which are the 2-(furan-2-yl) analogues of **3-11**, respectively. The furan-2-yl group seemed the ideal substituent at this position to obtain good affinity at all three receptors. In fact, hA_1, hA_{2A}, and hA_3 ARs binding affinities of **12-20** were comparable to or higher than those of the corresponding 2-phenyl derivatives **3-11** with the only exception being the hA_3 AR affinity of **19** which is 35-fold lower than that of compound **10**. This trend was expected since the furan-2-yl ring at this position is a profitable substituent in other classes of AR antagonists and in our 5,7-diaminothiazolo[5,4-d]pyrimidine derivatives. [34, 18, 32, 33]

It has to be noted that in the 2-(furan-2-yl)-5-aryl derivatives **13-18**, differently from what was observed in the corresponding 2-phenyl derivatives **4-9**, the presence and nature of the substituents on the appended 5-phenyl ring seem to have no influence on the binding activity at the hA_{2A} AR. In fact, all the 2-(furan-2-yl)-5-aryl substituted derivatives **13-18** showed a comparable binding affinity falling in the nanomolar range. On the contrary, looking at the hA_1 and hA_3 AR binding results of **13-18** we observed the same trend of the corresponding 2-phenyl derivatives **3-9**. In fact,

the best substituent for both hA_1 and hA_3 AR affinities is still the 3-hydroxymethyl one, derivative **13** being the most active at these two hARs (hA_1 K_i = 28 nM; hA_3 K_i = 0.9 nM).

It has to be noted that the 2,5-difuran-2-yl derivative **19** in addition to be highly hA_{2A} vs hA_1 selective, such as the corresponding 2-phenyl-5-(furan-2-yl) **10**, it has also the best selectivity vs the hA_3 subtype. A similar behavior can be observed for the 5-(methylfuran-2-yl)-2-furan-2-yl **20** with respect to its corresponding 5-(methylfuran-2-yl)-2-phenyl **11**. In fact, compound **20** is A_{2A} selective vs the A_1 AR and showed a hA_{2A} binding affinity about 6-fold higher compared to that at the hA_3 ARs subtype, whereas the corresponding 2-phenyl derivative **11** is a non-selective ligand.

Derivatives **9**, **10**, **18** and **19**, able to bind hA_{2A} ARs with nanomolar affinity and a good degree of selectivity were chosen to be tested for their antagonistic properties by evaluating their effect on cAMP production in CHO cells, stably expressing the hA_{2A} AR. The obtained results (Table 2) showed that the compounds behaved as antagonists as they were able to counteract NECA-stimulated cAMP accumulation.

Table 2. Potencies of compounds **9**, **10**, **18**, and **19** at hA_{2A} AR.

	hA_{2A} AR IC_{50} (nM)[a]
9	627 ± 114
10	163 ± 41
18	764 ± 132
19	301 ± 82

[a]IC_{50} values obtained by inhibition of NECA-stimulated adenylyl cyclase activity in CHO cells expressing hA_{2A} AR.

Table 3 reports the binding affinities at hA_1, hA_{2A} and hA_3 ARs of derivatives **21-27** which were obtained by introduction of different acyl groups on the 7-amino function of the parents **2, 3** and **12**. This modification was performed in order to shift affinity and selectivity toward the hA_3 receptor

subtype. As expected, this structural modification, in general, afforded an increase in the hA_3 binding, depending on the nature of the acyl group.

Table 3. Binding affinity of compounds **21-27** at hA_1, hA_{2A} and hA_3 ARs.[a]

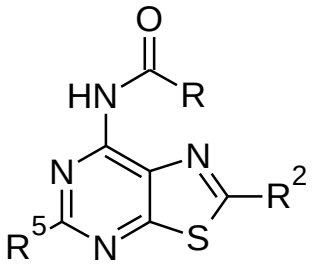

21-27

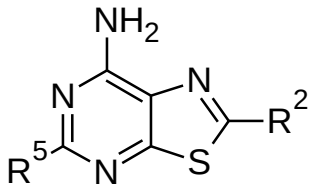

2, 3, 12

	R^2	R^5	R	binding experiments K_i (nM)			A_3 selectivity	
				hA_1[b]	hA_{2A}[c]	hA_3[d]	A_1/A_3	A_{2A}/A_3
2	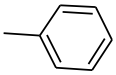		/	34 ± 1	248 ± 33	2656 ± 235	0.01	0.09
21			C_6H_5	935 ± 82	1951 ± 209	691 ± 118	1.3	2.8
22			4Cl-C_6H_4	>30000	>30000	>30000		
23			4OCH_3-C_6H_5	1461 ± 243	>30000	91 ± 12	16	>300
3	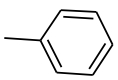	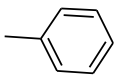	/	148 ± 16	19 ± 6.2	84 ± 13	1.76	0.22
24			C_6H_5	1472 ± 273	104 ± 210	1199 ± 286	1.2	0.08
25			furan-2-yl	2275 ± 1242	3980 ± 1692	48 ± 1.2	47.4	83
12	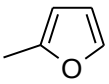	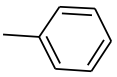	/	33 ± 2	3 ± 0.04	15 ± 2.9	2.2	0.2
26			C_6H_5	>30000	1144 ± 278	32 ± 3.2	>900	35.7
27			furan-2-yl	265 ± 63	428 ± 12	4 ± 0.51	66.2	107

[a]Data (n = 3−5) are expressed as means ± standard errors. [b]Displacement of specific [^{3}H]-CCPA binding at hA_1 AR expressed in CHO cells. [c]Displacement of specific [^{3}H]-NECA binding at hA_{2A} AR expressed in CHO cells. [d]Displacement of specific [^{3}H]-HEMADO binding at hA_3 AR expressed in CHO cells.

In fact, the best combination for hA_3 affinity and selectivity is a furoylamine function at position 7 together with a furan-2-yl and a phenyl moiety at positions 2 and 5, respectively (see compound **27**

hA_3 K_i = 4 nM). Analyzing the results, we observe that introduction of an acyl group is always detrimental for the hA_1 and hA_{2A} binding activity. This is in accordance with previously reported data on our bicyclic analogues confirming that the free 7-amino group is important for the anchoring of the ligand at the A_1 and A_{2A} subtypes [28].

Molecular docking analyses were performed to simulate the binding mode of the synthesized compounds at the hA_{2A} AR cavity. As molecular target, we chose the high-resolution crystal structure of the hA_{2A} AR in complex with the antagonist/inverse agonist 4-(2-(7-amino-2-(furan-2-yl)[1,2,4]triazolo[2,3-a][1,3,5]triazin-5-ylamino)ethyl)phenol (ZM241385) (http://www.rcsb.org; pdb code: 5NM4; 1.7-Å resolution [35]). MOE (Molecular Operating Environment 2014.09 [36]) docking tool ("induced fit" setting) and Gold [37] and Autodock software [38, 39] were employed for this task. Analogously to a previous study at the same receptor [24], we performed docking analyses with various docking tools to get a sort of average binding mode prediction of the synthesized compounds at the hA_{2A} AR binding cavity.

According to docking results, the synthesised molecules **2-20** get inserted into the binding site of the hA_{2A} AR with the thiazolo[5,4-d]pyrimidine scaffold located analogously to the triazolo-triazine core of the co-crystallized derivative ZM241385. Even the ligand-target interactions appear conserved with respect to the co-crystallized ligand, as the new compounds generally engage a double H-bond interaction with the Asn253$^{6.55}$ side chain (through the N1 atom and the 7-amine function) and an additional polar contact with Glu169 (EL2). Further key interactions are a π-π interaction with Phe168 (EL2) and a non-polar interaction with the Leu249$^{6.51}$ side chain (Fig. 2). The 5-substituent points toward the extracellular environment and gets in proximity to Ile66$^{2.64}$, Ser67$^{2.65}$, Leu167 (EL2), Glu169 (EL2), Leu267 (EL3), and Tyr271$^{7.36}$, while the 2-substituent is inserted into the depth of the binding cavity, in proximity to residues belonging to TM3, TM5 and TM6 segments (Val84$^{3.32}$, Leu85$^{3.33}$, Thr88$^{3.36}$, Met177$^{5.38}$, Trp246$^{6.48}$, Leu249$^{6.51}$, His250$^{6.52}$, and Asn253$^{6.55}$).

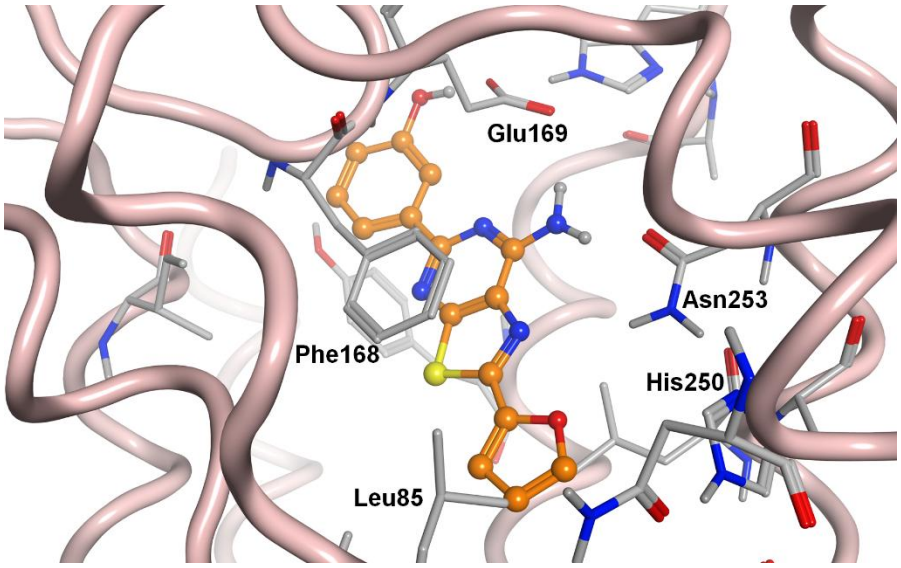

Figure 2. The general binding mode of the synthesized compounds at the hA_{2A} AR cavity, according to docking-scoring results; compound **18** is represented and key receptor residues are indicated.

The 5-substituent is generally a substituted phenyl group, where the substituents on this ring modulate the affinity for the three ARs. In particular, compounds bearing meta-substituents are endowed with higher hA_{2A} AR affinity with respect to compounds presenting the same substituents at the para-position. **Figure 3A** shows a top-view of the compound binding mode with the hA_{2A} AR residues in proximity to the 5-substituent. Polar groups at the meta-position of the 5-phenyl ring are able to engage H-bond interactions with H-bond functions of the receptor, like the backbone NH groups of Phe168 and Glu169 (EL2) and the hydroxyl group of Tyr271$^{7.36}$. Additional interactions may be given with Ile66$^{2.64}$, Ser67$^{2.65}$, Leu167 (EL2), and Leu267 (EL3) residues. For the 2,5-diphenyl derivative **3**, the replacement of the 5-unsubstituted phenyl ring with a furan-2-yl moiety (**10**) affords a significant improvement of affinity. Docking results showed that compounds bearing at least one furan-2-yl substituent are located in the binding cleft with this group inserted into the depth of the cavity. In fact, the binding mode of 5-(furan-2-yl)-2-phenyl derivative **10** is a mirror-version of the generally observed docking conformations (see above), with the 5-substituent (i.e. furan-2-yl group) deeply inserted into the cavity and the 2-substituent (i.e. phenyl group) pointing

toward the external environment. Compounds bearing two furan-2-yl groups (i.e. **19**) may be inserted in both arrangements, according to docking results.

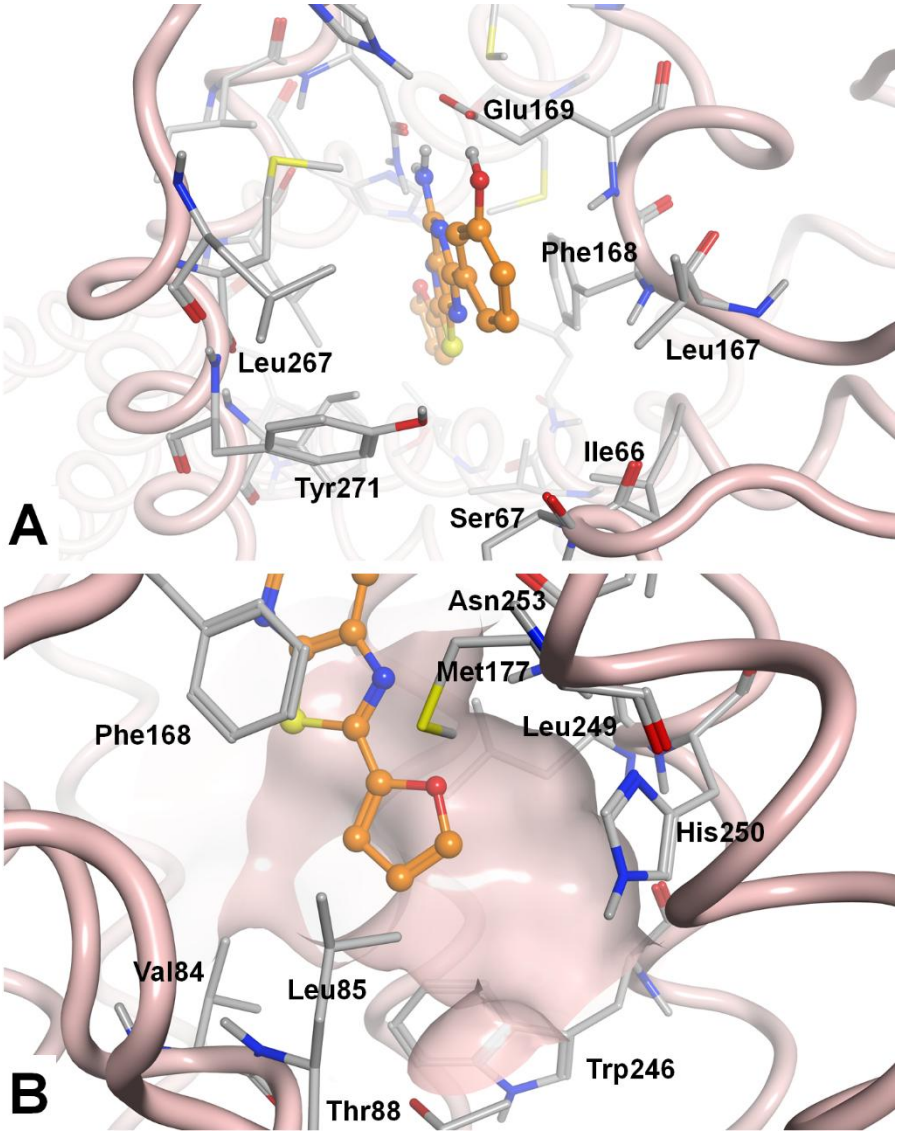

Figure 3. A. Top view of the docking conformation of compound **18** at the hA_{2A} AR; the key residues for the interaction with 5-substituent are indicated. **B.** Detail of the depth of the hA_{2A} AR binding cavity, represented as molecular surface. In this cavity is generally located the 2-substituent. The residues indicated are the ones in the closest proximity to the 2-substituent and have been considered for the calculation of the interaction forces with the svl *IF-E 6.0* tool (see in main text).

It is generally observed at the hA_{2A} AR that compounds presenting a furan-2-yl substituent into the depth of the binding cavity (in proximity of Asn253$^{6.55}$) are endowed with higher affinity with respect to those presenting a phenyl ring in the same position. Docking studies of compounds **2-20** showed that the substituent inserted in this region is the one bound to the C2 atom of the bicyclic core. Moreover, binding data reported in Table 1 indicated that compounds bearing a furan-2-yl group as 2-substituent (compounds **12-20**) are endowed with higher affinity with respect to the corresponding derivatives bearing a 2-phenyl substituent (compounds **3-11**). To justify this trend, we performed a post-docking analysis of the interactions between the compounds and the receptor binding site by using the *IF-E 6.0* [40] tool that is retrievable at the SVL exchange service (Chemical Computing Group, Inc. SVL exchange: http://svl.chemcomp.com). This tool was previously employed for other analyses at ARs [26, 29, 41]. The script calculates atomic and residue interaction forces and displays them as 3D vectors. Furthermore, it calculates the per-residue interaction energies (values in kcal/mol), where negative and positive energy values are associated to favorable and unfavourable interactions, respectively. Hence, for this task we employed three pairs of compounds (**14** and **5**, **16** and **7**, **18** and **9**) bearing the same substituent at the 5-position, and a furan-2-yl or a phenyl ring as 2-substituent. The results of this analysis are reported in Table 4.

Table 4. Interaction energies (values in kcal/mol) between 2-(furan-2-yl) derivatives (**14**, **16**, **18)** and 2-phenyl derivatives (**5**, **7**, **9)** and the binding site residues located in proximity of the 2-position of the analyzed compounds. See text for details.

	14	**5**	**16**	**7**	**18**	**9**
Val84	0,01	-0,28	-0,24	-0,41	-0,52	-0,36
Leu85	-1,52	-1,42	-1,32	-1,25	-1,51	-1,38
Thr88	-0,73	-1,23	-0,82	-1,31	-1,04	-1,36
Phe168	-6,48	-6,80	-6,30	-5,87	-6,38	-6,53

Met177	-1,52	-1,47	-1,76	-1,62	-1,89	-1,68
Trp246	-0,10	0,20	0,02	0,43	0,44	0,45
Leu249	-2,27	-1,45	-2,68	-1,40	-2,97	-0,94
His250	-2,65	-4,15	-2,43	-4,15	-2,09	-3,64
Asn253	-11,09	-8,79	-11,05	-9,12	-9,94	-8,60
tot	*-26,35*	*-25,39*	*-26,58*	*-24,70*	*-25,90*	*-24,04*

From the results reported in Table 4 it may be observed that the sum of contributes of aminoacids located in proximity of the 2-substituent appears favorable for compounds bearing a furan-2-yl group in this position with respect to those bearing a phenyl ring at the same position. The polar interaction between the oxygen atom of the furan-2-yl substituent and the side chain of Asn253$^{6.55}$ represents the strongest ligand-target interaction. Substitution of the furan-2-yl moiety with a phenyl ring makes this polar contact impossible, leading to a lower interaction.

Docking experiments were also performed at a hA_1 AR crystal structure (pdb code: 5UEN; 3.2-Å resolution [42]) with the same docking tools and protocols as above. Docking conformations obtained at this receptor model appear quite in agreement with the ones observed at the hA_{2A} AR (see Fig. 4A). Interactions between compounds **2-20** and the hA_{2A} and hA_1 ARs are generally conserved, and this could explain the similar nanomolar affinity data at these two ARs, even if the affinity at the hA_1 AR appears generally lower for all compounds respect to the one at the hA_{2A} AR. Comparing the hA_1 AR and hA_{2A} AR docking data, it appears that some residues at the entrance of the hA_1 AR binding cavity (Glu170, Ser267, and Tyr271$^{7.36}$, Fig. 4B) and in proximity to the 5-substituents are different in some cases with respect to the corresponding ones in the hA_{2A} AR (Leu167, Leu267, and Tyr271$^{7.36}$). In particular, the hA_1 AR presents a set of charged residues in proximity to the 5-substituent and these aminoacids make an inter-residue polar interaction network (Fig. 4B). This could be one of the factors leading to a slightly different interaction with the

compounds with respect to the hA_{2A} AR subtype that presents in the same region a set of less polar aminoacids.

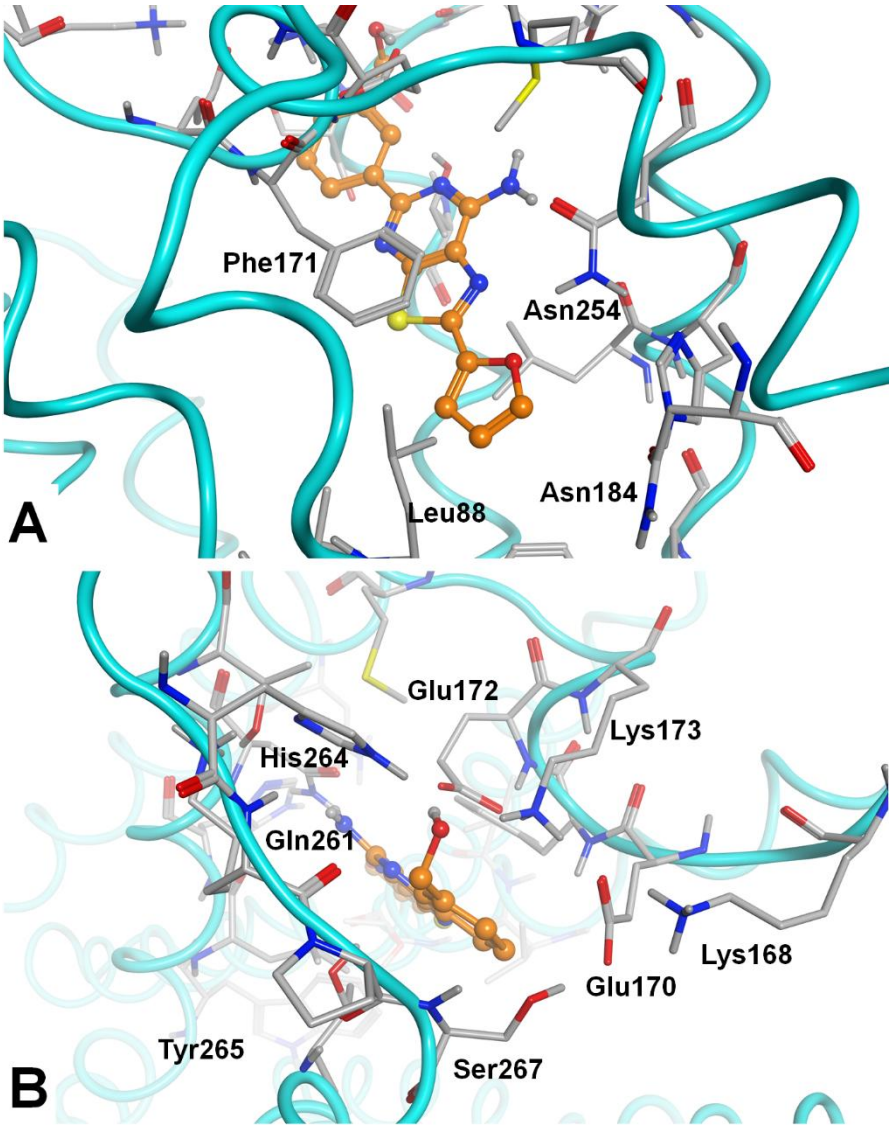

Figure 4. A The general binding mode of the synthesized compounds at the hA_1 AR cavity, according to docking-scoring results; compound **13** is represented and key receptor residues are indicated. **B.** Top view of the docking conformation of compound **13** at the hA_1 AR; the key residues for the interaction with 5-substituent are indicated.

Docking experiments were also performed (with the same settings) at a homology model of the hA_3 AR [24], obtaining analogue docking conformations with respect to the ones observed at the hA_{2A} AR and hA_1 AR (Fig. 5A). As described above, the interactions between compounds and the binding cavity are quite conserved among these three AR subtypes, apart from some small

differences, which are located at the entrance of these receptor regions. The residues of this region of the hA_3 AR are not particularly polar, with only one charged residue (the EL3 residue Glu258). Similarly, the hA_{2A} AR presents Glu169 (EL2) as the sole charged residue. Instead, the hA_1 AR shows several charged residues (see above), hence a significantly different chemical-physical profile at this receptor region can be noted. Moreover, the hA_3 AR has two aminoacids able to engage H-bond interactions (Gln167 in EL2 and Gln261 in EL3, Fig. 5B) with the 5-substituent, similarly to some H-bond functions present at the entrance of the hA_{2A} AR cavity (see above). These similarities could help interpret the comparable trend of affinities of compounds for the hA_{2A} and hA_3 ARs.

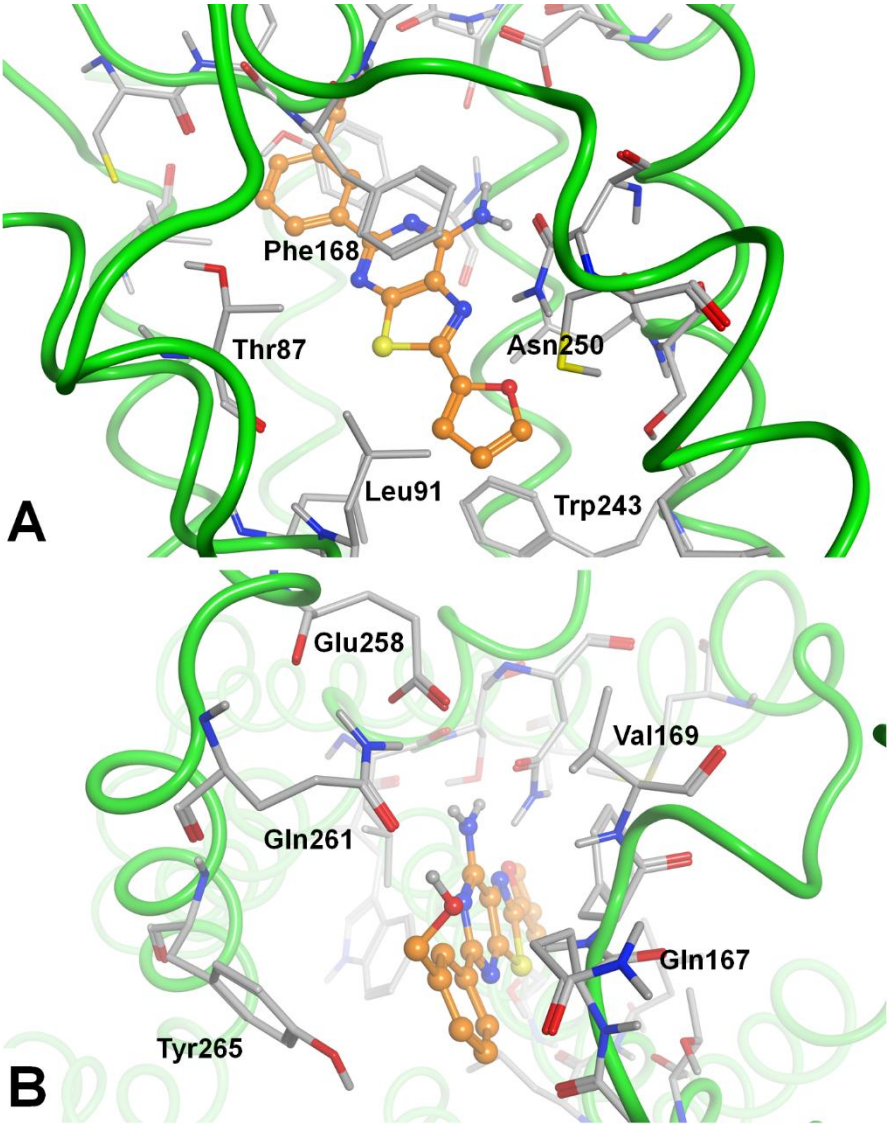

Figure 5. A The general binding mode of the synthesized compounds at the hA_3 AR cavity, according to docking-scoring results; compound **13** is represented and key receptor residues are indicated. **B.** Top view of the docking conformation of compound **13** at the hA_3 AR; the key residues for the interaction with 5-substituent are indicated.

In conclusion, the simplicity of the synthetic processes and the decoration capability of the 7-aminothiazolo[5,4-d]pyrimidine core make it a privileged structure for the design of novel AR ligands with distinct selectivity profiles for the AR subtypes. The obtained results allowed us to conclude that affinity and/or selectivity of the 7-aminothiazolo[5,4-d]pyrimidines towards ARs can be modulated by the nature of the substituents attached at positions 2, 5 and 7 of the bicyclic scaffold. For instance, the presence of a furan-2-yl in both the 2 and 5 positions produces the best combination of hA_{2A} AR affinity and selectivity (compound **19**). Moreover, two derivatives (compounds **4** and **5**) bearing a phenyl and aryl moieties at positions 2 and 5, respectively, and possessing nanomolar affinity and good selectivity for the hA_3 AR subtype, were identified. As expected, substitution of the 7-amino group with acyl moieties was profitable for the anchoring at the hA_3 AR subtype (i.e. compound **27**). Additionally, molecular docking simulations have been supportive to rationalize the observed affinity data at the hA_{2A}, hA_1 and hA_3 AR structures.

Author Contributions

All authors have given approval to the final version of the manuscript.

Notes

The authors declare no competing financial interest.

Acknowledgment

The synthetic work was financially supported by the University of Florence and the Italian Ministry for University and Research (MIUR, PRIN 2010-2011, 20103W4779_004 project).

References.

1. Borea PA, Gessi S, Merighi S, Vincenzi F, Varani K. Pharmacology of adenosine receptors: the state of the art. *Physiol. Rev.* 2018; 98:1591-1625.

2. Borea PA, Gessi S, Merighi S, Varani K. Adenosine as a multi-signalling guardian angel in human diseases: when, where and how does it exert its protective effects? *Trends Pharmacol. Sci.* 2016; 37:419-434.

3. Gessi S, Merighi S, Varani K, Borea PA. Adenosine receptors in health and disease. *Adv. Pharmacol.* 2011; 61:41-75.

4. Varani K, Vincenzi F, Merighi S, Gessi S, Borea PA. Biochemical and pharmacological role of A_1 adenosine receptors and their modulation as novel therapeutic strategy. *Adv. Exp. Med. Biol.- Protein Reviews* 2017; 19:193-232.

5. Mitrovic V, Seferovic P, Dodic S, Krotin M, Neskovic A, Dickstein K, Voogd HDE, Bocker C, Ziegler D, Godes M, Nakov R, Essers H, Verboom C, Hocher B. Cardio-renal effects of the A_1 adenosine receptor antagonist SVL320 in patients with heart failure. *Circ. Hear. Fail.* 2009; 2:523-531.

6. Yap SC, Lee HT. Adenosine and protection from acute kidney injury. *Curr. Opin. Nephrol. Hypertens.* 2012; 21:24-32.

7. Mihara T, Mihara K, Yarimizu J, Mitani Y, Matsuda R, Yamamoto H, Aoki S, Akahane A, Iwashita A, Matsuoka N. Pharmacological characterization of a novel, potent adenosine A_1 and A_{2A} receptor dual antagonist, 5-[5-amino-3-(4-fluorophenyl)pyrazine-2-yl]-1-isopropylpyridine-2(1H)-one (ASP5854), in models of Parkinson's disease and cognition. *J. Pharmacol. Exp. Ther.* 2007; 323:708-719.

8. Preti D, Baraldi PG, Moorman AR, Borea PA, Varani K. History and perspectives of A_{2A} adenosine receptor antagonists as potential therapeutic agents. *Med. Res. Rev.* 2015; 35:790-848.

9. Jenner P. An overview of adenosine A_{2A} receptor antagonists in Parkinson's disease. *Int. Rev. Neurobiol.* 2014; 119:71-86.

10. Fernández P, Trzaska S, Wilder T, Chiriboga L, Blackburn MR, Cronstein BN, Chan ES. Pharmacological blockade of A_{2A} receptors prevents dermal fibrosis in a model of elevated tissue adenosine. *Am. J. Pathol.* 2008; 172:1675-1682.

11. Perez-Aso M, Fernandez P, Mediero A, Chan ES, Cronstein BN. Adenosine A_{2A} receptor promotes collagen production by human fibroblasts via pathways involving cyclic AMP and AKT but independent of Smad2/3. *FASEB J.* 2014; 28:802-812.

12. Perez-Aso M, Mediero A, Low YC, Levine J, Cronstein BN. Adenosine A_{2A} receptor plays an important role in radiation-induced dermal injury. *FASEB J.* 2016; 30:457-465.

13. Boia R, Ambrosio AF, Santiago AR. Therapeutic opportunities for caffeine and A_{2A} receptor antagonists in retinal diseases. *Ophthalmic Res.* 2016; 55:212-218.

14. Vijayan D, Young A, Teng MWL, Smyth MJ. Targeting immunosuppressive adenosine in cancer. *Nat. Rev. Cancer*. 2017; 17:709-724.

15. Ohta A, Gorelik E, Prasad SJ, Ronchese F, Lukashev D, Wong MK, Huang X, Caldwell S, Liu K, Smith P, Chen JF, Jackson EK, Apasov S, Abrams S, Sitkovsky M. A_{2A} adenosine receptor protects tumors from antitumor T cells. *Proc. Natl. Acad. Sci. U. S. A.* 2006; 103:13132-13137.

16. Young A, Ngiow SF, Gao Y, Patch AM, Barkauskas DS, Messaoudene M, Lin G, D. Coudert JD, Stannard KA, Zitvogel L, Degli-Esposti MA, Vivier E, Waddell N, Linden J, Huntington ND, Souza-Fonseca-Guimaraes F, Smyth MJ. A_{2A}R adenosine signaling suppresses natural killer cell maturation in the tumor microenvironment. *Cancer Res.* 78 2018; 78:1003-1016.

17. Gessi S, Bencivenni S, Battistello E, Vincenzi F, Colotta V, Catarzi D, Varano F, Merighi S, Borea PA, Varani K. Inhibition of A_{2A} adenosine receptor signaling in cancer cells proliferation by the novel antagonist TP455. *Front. Pharmacol.* 2017; 8:888.

18. Varano F, Catarzi D, Vincenzi F, Betti M, Falsini M, Ravani A, Borea PA, Colotta V, Varani K. Design, synthesis and pharmacological characterization of 2-(2-furanyl)thiazolo[5,4-d]pyrimidine-5,7-diamine derivatives: new highly potent A_{2A} adenosine receptor inverse agonists with antinociceptive activity. *J. Med. Chem.* 2016; 59:10564-10576.

19. Zablocki J, Elzein E, Kalla R. A_{2B} adenosine receptor antagonists and their potential indications. *Expert Opin. Ther. Pat.* 2006; 16:1347-1357.

20. Baraldi PG, Preti D, Borea PA, Varani K. Medicinal chemistry of A_3 adenosine receptor modulators: pharmacological activities and therapeutic implications. *J. Med. Chem.* 2012; 55:5676-5703.

21. Borea PA, Varani K, Vincenzi F, Baraldi PG, Tabrizi MA, Merighi S, Gessi S. The A_3 adenosine receptor: history and perspectives. *Pharmacol. Rev.* 2015; 67:74-102.

22. Jacobson KA, Merighi S, Varani K, Borea PA, Baraldi S, Tabrizi MA, Romagnoli R, Baraldi PG, Ciancetta A, Tosh DK, Gao ZG, Gessi S. A_3 adenosine receptors as modulators of inflammation: from medicinal chemistry to therapy. *Med. Res. Rev.* 2017:1-42.

23. Poli D, Falsini M, Varano F, Betti M, Varani K, Vincenzi F, Pugliese AM, Pedata F, Dal Ben D, Thomas A, Palchetti I, Bettazzi F, Catarzi D, Colotta V. Imidazo[1,2-a]pyrazin-8-amine core for the design of new adenosine receptor antagonists: structural exploration to target the A_3 and A_{2A} subtypes. *Eur. J. Med. Chem.* 2017; 125:611-628.

24. Falsini M, Squarcialupi L, Catarzi D, Varano F, Betti M, Dal Ben D, Marucci G, Buccioni M, Volpini R, De Vita T, Cavalli A, Colotta V. The 1,2,4-triazolo[4,3-a]pyrazin-3-one as a versatile scaffold for the design of potent adenosine human receptor antagonists. Structural investigations to target the A_{2A} receptor subtype. *J. Med. Chem.* 2017; 60:5772-5790.

25. Squarcialupi L, Catarzi D, Varano F, Betti M, Falsini M, Vincenzi F, Ravani A, Ciancetta A, Varani K, Moro S, Colotta V. Structural refinement of pyrazolo[4,3-d]pyrimidine derivatives to obtain highly potent and selective antagonists for the human A_3 adenosine receptor. *Eur. J. Med. Chem.* 2016; 108:117-133.

26. Squarcialupi L, Falsini M, Catarzi D, Varano F, Betti M, Varani K, Vincenzi F, Dal Ben D, Lambertucci C, Volpini R, Colotta V. Exploring the 2- and 5-positions of the pyrazolo[4,3-d]pyrimidin-7-amino scaffold to target human A_1 and A_{2A} adenosine receptors. *Bioorg. Med. Chem.* 2016; 24:2794-2808.

27. Catarzi D, Varano F, Poli D, Squarcialupi L, Betti M, Trincavelli L, Martini C, Dal Ben D, Thomas A, Volpini R, Colotta V. 1,2,4-Triazolo[1,5-a]quinoxaline derivatives and their simplified analogues as adenosine A_3 receptor antagonists. Synthesis, structure-affinity relationships and molecular modeling studies. *Bioorg. Med. Chem.* 2015; 23:9-21.

28. Squarcialupi L, Colotta V, Catarzi D, Varano F, Filacchioni G, Varani K, Corciulo C, Vincenzi F, Borea PA, Ghelardini C, Di Cesare Mannelli L, Ciancetta A, Moro S. 2-Arylpyrazolo[4,3-d]pyrimidin-7-amino derivatives as new potent and selective human A_3

adenosine receptor antagonists. Molecular modeling studies and pharmacological evaluation. *J. Med. Chem.* 2013; 56:2256-2269.

29. Varano F, Catarzi D, Squarcialupi L, Betti M, Vincenzi F, Ravani A, Varani K, Dal Ben D, Thomas A, Volpini R, Colotta V. Exploring the 7-oxo-thiazolo[5,4-d]pyrimidine core for the design of new human adenosine A_3 receptor antagonists. Synthesis, molecular modeling studies and pharmacological evaluation. *Eur. J. Med. Chem.* 2015; 96:105-121.

30. Colotta V, Catarzi D, Varano F, Cecchi L, Filacchioni G, Martini C, Trincavelli L, Lucacchini A. 1,2,4-Triazolo[4,3-a]quinoxalin-1-one: a versatile tool for the synthesis of potent and selective adenosine receptor antagonists. *J. Med Chem.* 2000; 43:1158-1164.

31. Colotta V, Catarzi D, Varano F, Calabri FR, Lenzi O, Filacchioni G, Martini C, Trincavelli L, Deflorian F, Moro S. The 1,2,4-triazolo[4,3-a]quinoxalin-1-one moiety as an attractive scaffold to develop new potent and selective human A_3 adenosine receptor antagonists: synthesis, pharmacological and ligand-receptor modeling studies. *J. Med. Chem.* 2004; 47:3580-3590.

32. Varano F, Catarzi D, Vincenzi F, Falsini M, Pasquini S, Borea PA, Colotta V, Varani K. Structure-activity relationship studies and pharmacological characterization of N^5-heteroarylalkyl-substituted-2-(2-furanyl)thiazolo[5,4-d]pyrimidine-5,7-diamine-based derivatives as inverse agonists at human A_{2A} adenosine receptor. *Eur. J. Med. Chem.* 2018; 155:552-561.

33. Varano F, Catarzi D, Falsini M, Vincenzi F, Pasquini S, Varani K, Colotta V. Identification of novel thiazolo[5,4-d]pyrimidine derivatives as human A_1 and A_{2A} adenosine receptor antagonists/inverse agonists. *Bioorg. Med. Chem.* 2018; 26:3688-3695.

34. de Lera Ruiz M, Lim YH, Zheng J. Adenosine A_{2A} receptor as a drug discovery target. *J. Med. Chem.* 2014; 57:3623-3650.

35. Weinert T, Olieric N, Cheng R, Brunle S, James D, Ozerov D, Gashi D, Vera L, Marsh M, Jaeger K, Dworkowski F, Panepucci E, Basu S, Skopintsev P, Dore AS, Geng T, Cooke RM, Liang M, Prota AE, Panneels V, Nogly P, Ermler U, Schertler G, Hennig M, Steinmetz MO, Wang M, Standfuss J. Serial millisecond crystallography for routine room-temperature structure determination at synchrotrons. *Nat. Commun.* 2017; 8(1):542.

36. Molecular Operating Environment, C.C.G., Inc., 1255 University St., Suite 1600, Montreal, Quebec, Canada, H3B 3X3;

37. Jones G, Willett P, Glen RC, Leach AR, Taylor R. Development and validation of a genetic algorithm for flexible docking. *J. Mol. Biol.* 1997; 267(3):727-748.

38. Morris GM, Goodsell DS, Halliday RS, Huey R, Hart WE, Belew RK, Olson AJ. Automated docking using a Lamarckian genetic algorithm and an empirical binding free energy function. *J. Comput. Chem.* 1998; 19:1639-1662.

39. Morris GM, Huey R, Lindstrom W, Sanner MF, Belew RK, Goodsell DS, Olson AJ. AutoDock4 and AutoDockTools4: Automated docking with selective receptor flexibility. *J. Comput. Chem.* 2009; 30:2785-2791.

40. Shadnia H, Wright JS, Anderson JM. Interaction force diagrams: new insight into ligand-receptor binding. *J. Comput. Aided Mol. Des.* 2009; 23:185-194.

41. Dal Ben D, Buccioni M, Lambertucci C, Marucci G, Thomas A, Volpini R, Cristalli G. Molecular modeling study on potent and selective adenosine A_3 receptor agonists. *Bioorg. Med. Chem.* 2010; 18:7923-7930.

42. Glukhova A, Thal DM, Nguyen AT, Vecchio EA, Jorg M, Scammells PJ, May LT, Sexton PM, Christopoulos A. Structure of the adenosine A_1 receptor reveals the basis for subtype selectivity. *Cell* 2017; 168:867-877 e13.

Table(s)

Table 1. Binding affinity of compounds **2-20** at hA_1, hA_{2A} and hA_3 ARs.[a]

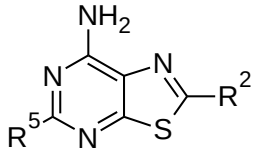

2-20

	R^2	R^5	binding experiments K_i (nM)			A_{2A} AR selectivity	
			hA_1[b]	hA_{2A}[c]	hA_3[d]	A_1/A_{2A}	A_3/A_{2A}
2	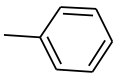	CH_3	34 ± 1	248 ± 33	2656 ± 235	0.14	10.7
3		C_6H_5	148 ± 16	19 ± 6.2	84 ± 13	7.8	4.4
4		C_6H_4-3-CH_2OH	32 ± 9	53 ± 13	3.7 ± 1.2	0.6	0.07
5		C_6H_4-4-CH_2OH	82 ± 17	82 ± 19	8.2 ± 0.5	1	0.1
6		C_6H_4-4-OCH_3	224.6 ± 61.3	115.3 ± 5.1	46.7 ± 12	1.9	0.4
7		C_6H_4-3-OCH_3	175.9 ± 34.7	109.8 ± 0.35	35.6 ± 9.2	1.6	0.3
8		C_6H_4-3-CN	594 ± 124	33.6 ± 8.9	247 ± 74	17.7	7.3
9		C_6H_4-3-OH	58.5 ± 6.1	5 ± 1.5	190 ± 16.7	11.7	38
10		furan-2-yl	67 ± 6.8	1.7 ± 0.2	2.8 ± 0.4	39.4	1.6
11		5-CH_3-furan-2-yl	28.9 ± 6.6	22.4 ± 4.03	24.9 ± 3.4	1.3	1.1
12	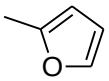	C_6H_5	33 ± 2	3 ± 0.04	15 ± 2.9	11	5
13		C_6H_4-3-CH_2OH	28 ± 5.5	2.1 ± 0.3	0.9 ± 0.1	13	0.4
14		C_6H_4-4-CH_2OH	77.7 ± 14.5	7.7 ± 0.45	3.58± 0.41	10.1	0.5
15		C_6H_4-4-OCH_3	47.7 ± 3.4	11.2 ± 0.83	4.66 ± 1.2	4.2	0.4
16		C_6H_4-3-OCH_3	62.3 ± 5.1	1.9 ± 0.33	4.90 ± 0.19	32.8	2.6
17		C_6H_4-3-CN	102.7 ± 6.8	7.7 ± 1.4	61.5 ±14.1	13.3	8.0
18		C_6H_4-3-OH	51.0 ± 1.6	1.64 ± 0.35	15.73 ± 3.5	31.1	9.6
19		furan-2-yl	69 ± 15	3.4 ± 0.9	99 ± 15	20.3	29.1
20		5-CH_3-furan-2-yl	45.9 ± 4.4	2.36 ± 0.4	13.76 ± 1.7	19.4	5.8

[a]Data (n = 3−5) are expressed as means ± standard errors. [b]Displacement of specific [^{3}H]-CCPA binding at hA_1 AR expressed in CHO cells. [c]Displacement of specific [^{3}H]-NECA binding at hA_{2A} AR expressed in CHO cells. [d]Displacement of specific [^{3}H]-HEMADO binding at hA_3 AR expressed in CHO cells.

Table(s)

Table 2. Potencies of compounds **9**, **10**, **18**, and **19** at hA_{2A} AR.

	hA_{2A} AR IC_{50} (nM)[a]
9	627 ± 114
10	163 ± 41
18	764 ± 132
19	301 ± 82

[a]IC_{50} values obtained by inhibition of NECA-stimulated adenylyl cyclase activity in CHO cells expressing hA_{2A} AR.

Table(s)

Table 3. Binding affinity of compounds **21-27** at hA_1, hA_{2A} and hA_3 ARs.[a]

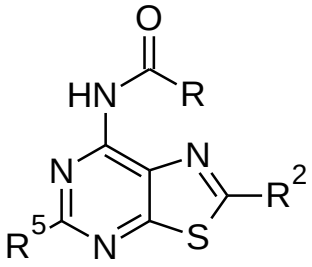

21-27

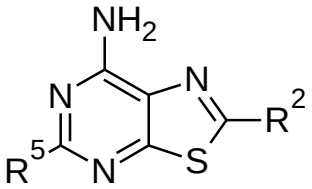

2, 3, 12

	R^2	R^5	R	binding experiments K_i (nM)			A_3 selectivity	
				hA_1[b]	hA_{2A}[c]	hA_3[d]	A_1/A_3	A_{2A}/A_3
2	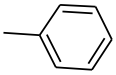		/	34 ± 1	248 ± 33	2656 ± 235	0.01	0.09
21			C_6H_5	935 ± 82	1951 ± 209	691 ± 118	1.3	2.8
22			4Cl-C_6H_4	>30000	>30000	>30000		
23			4OCH_3-C_6H_5	1461 ± 243	>30000	91 ± 12	16	>300
3	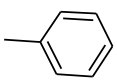	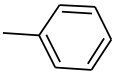	/	148 ± 16	19 ± 6.2	84 ± 13	1.76	0.22
24			C_6H_5	1472 ± 273	104 ± 210	1199 ± 286	1.2	0.08
25			furan-2-yl	2275 ± 1242	3980 ± 1692	48 ± 1.2	47.4	83
12	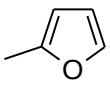	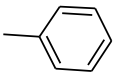	/	33 ± 2	3 ± 0.04	15 ± 2.9	2.2	0.2
26			C_6H_5	>30000	1144 ± 278	32 ± 3.2	>900	35.7
27			furan-2-yl	265 ± 63	428 ± 12	4 ± 0.51	66.2	107

[a]Data (n = 3−5) are expressed as means ± standard errors. [b]Displacement of specific [^{3}H]-CCPA binding at hA_1 AR expressed in CHO cells. [c]Displacement of specific [^{3}H]-NECA binding at hA_{2A} AR expressed in CHO cells. [d]Displacement of specific [^{3}H]-HEMADO binding at hA_3 AR expressed in CHO cells.

Figure(s)

Figure 1.

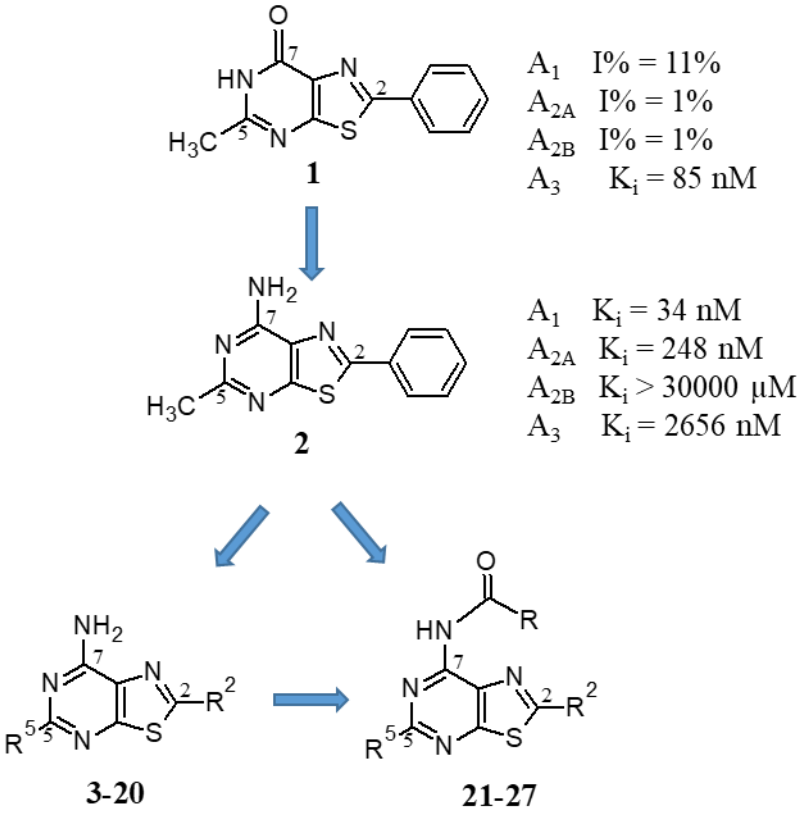

Figure(s)

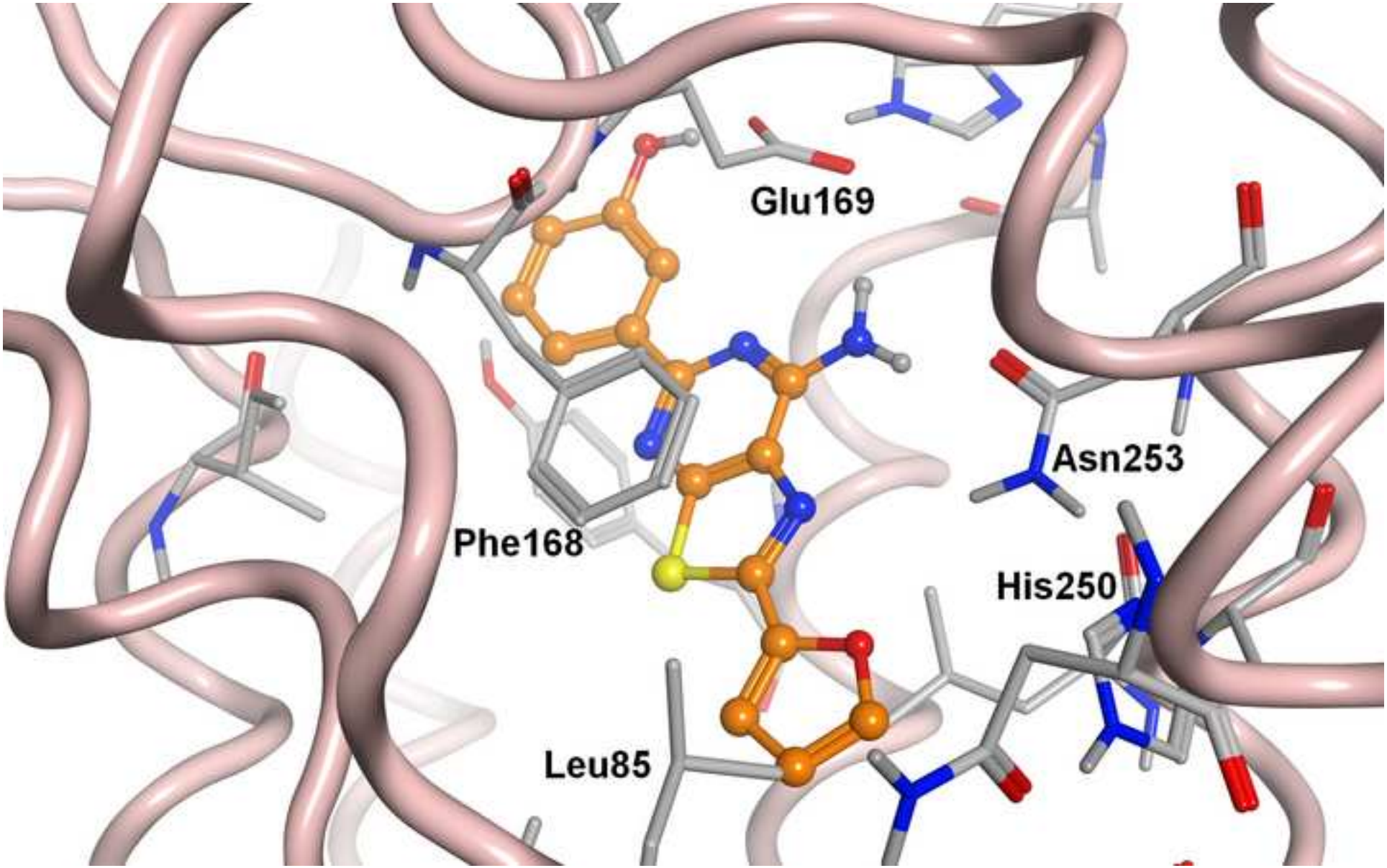

Figure(s)

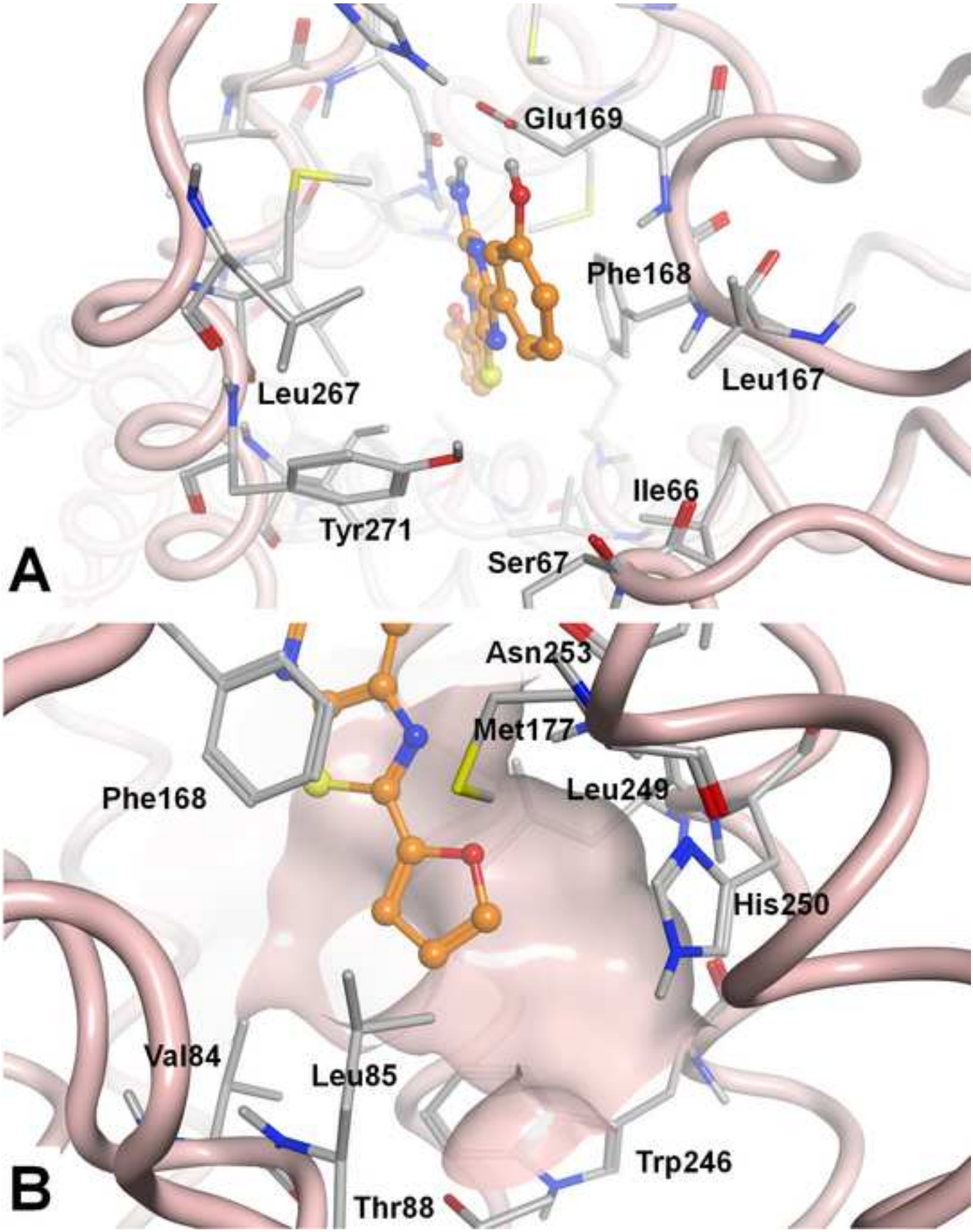
Glu169
Phe168
Leu167
Leu267
Tyr271
Ile66
Ser67
A
Asn253
Met177
Phe168
Leu249
His250
Val84
Leu85
Trp246
Thr88
B

Figure(s)

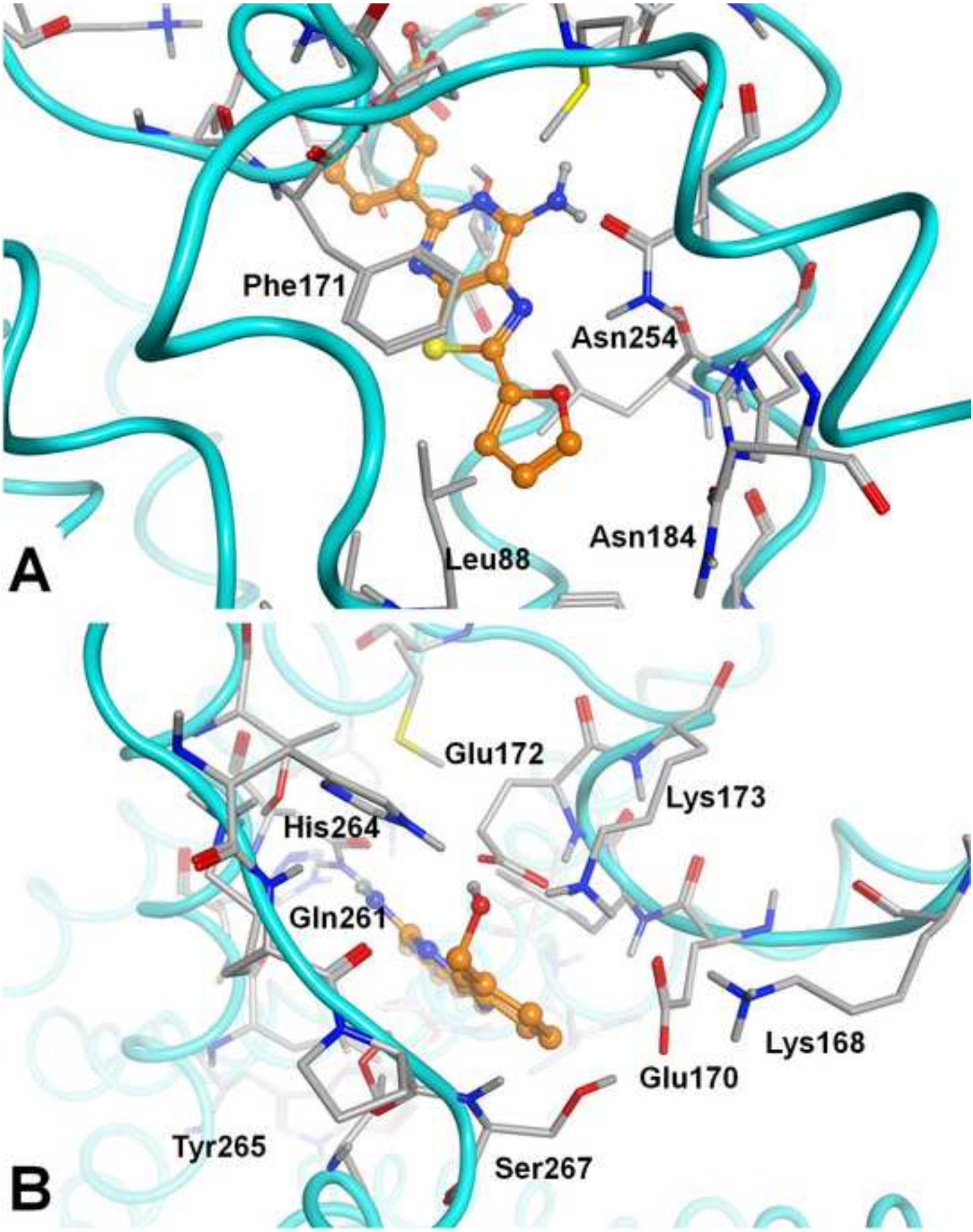
Phe171
Asn254
Asn184
Leu88
A
Glu172
Lys173
His264
Gln261
Lys168
Glu170
Tyr265
Ser267
B

Figure(s)

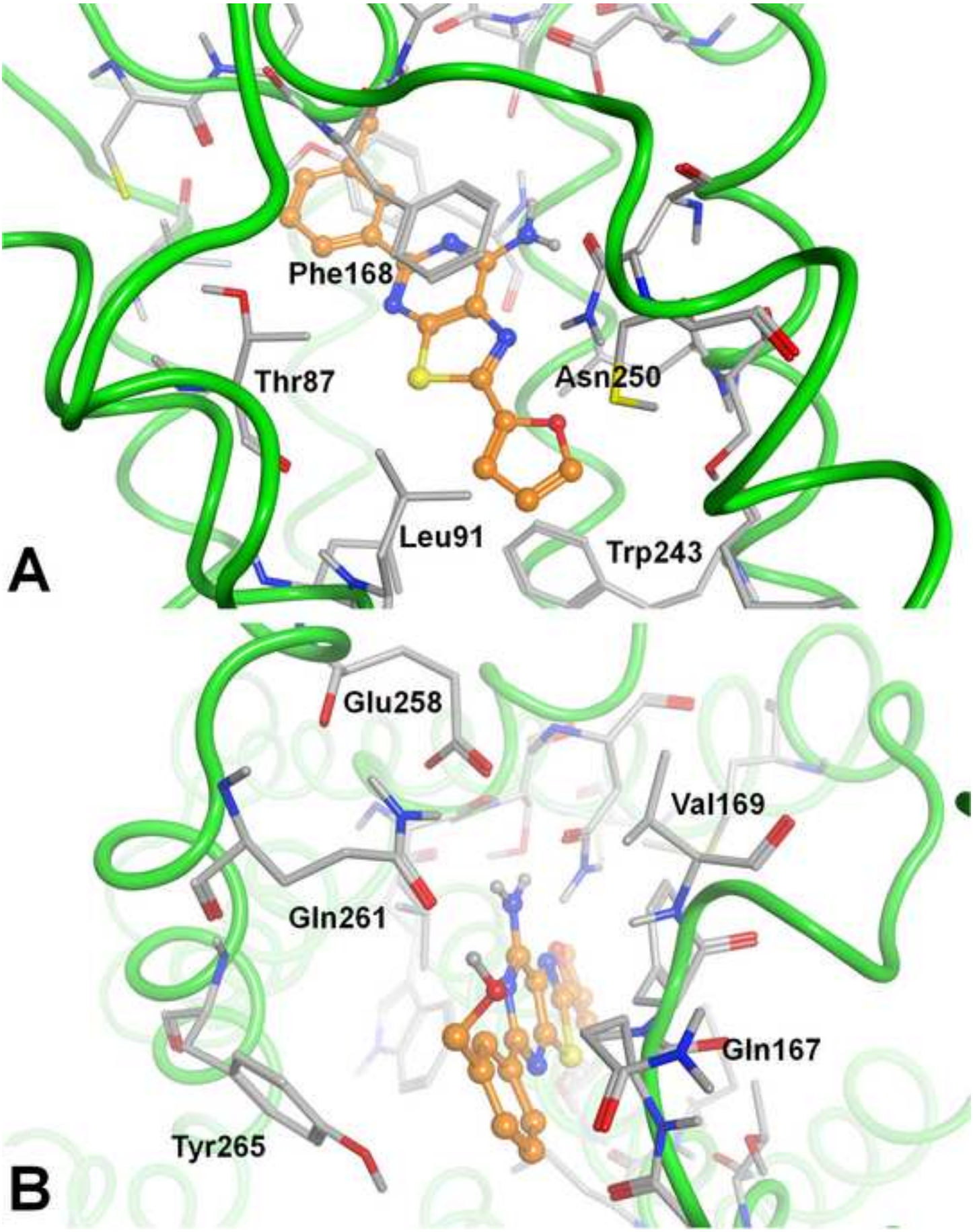
Phe168
Thr87
Asn250
Leu91
Trp243
A
Glu258
Val169
Gln261
Gln167
Tyr265
B

Figure(s)

Scheme 1

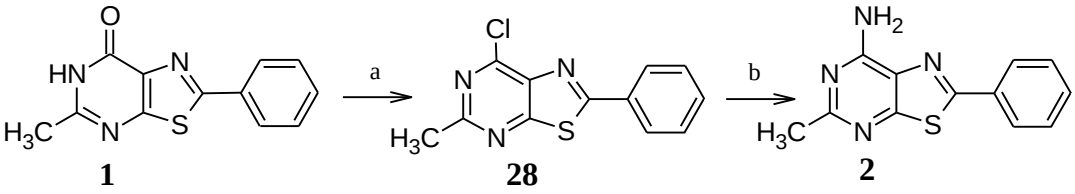

1 **28** **2**

Reagents and conditions: (a) $POCl_3$, dimethylaniline, reflux, 3h; (b) NH_3(g), EtOH, sealed tube, 130 °C, overnight, 95% yield.

Figure(s)

Schema 2.

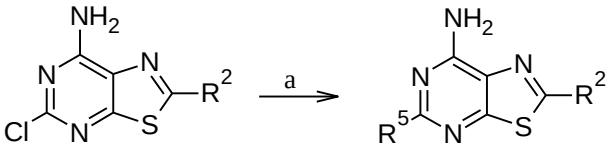

29 R^2 = phenyl
30 R^2 = furan-2yl

3-11 R^2 = phenyl
12-20 R^2 = furan-2yl

	R^5
3, 12	C_6H_5
4, 13	C_6H_4-3-CH_2OH
5, 14	C_6H_4-4-CH_2OH
6, 15	C_6H_4-4-OCH_3
7, 16	C_6H_4-3-OCH_3
8, 17	C_6H_4-3-CN
9, 18	C_6H_4-3-OH
10, 19	furan-2yl
11, 20	5-methylfuran-2yl

Reagents and conditions: (a) $R^5B(OH)_2$, tetrakis, Na_2CO_3, DME/H_2O, microwave irradiation, 160 °C 30 min (**3**-**4**, **6**-**7**, **12**-**13**, **17**-**18**), 35-68% yield, or reflux 4h (**5**, **8**-**11**, **14**-**16**, **19**-**20**), 30-72% yield.

Figure(s)

Scheme 3

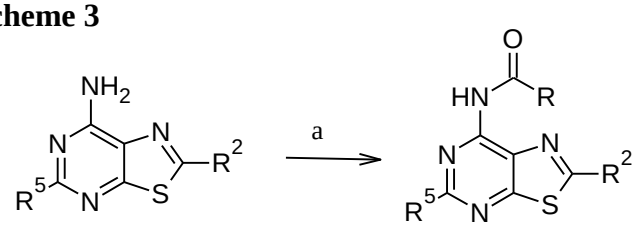

2 $R^2 = C_6H_5$ $R^5 = CH_3$

3 $R^2 = C_6H_5$ $R^5 = C_6H_5$

12 R^2 = furan-2yl $R^5 = C_6H_5$

21-23 $R^2 = C_6H_5$ $R^5 = CH_3$

24-25 $R^2 = C_6H_5$ $R^5 = C_6H_5$

26-27 R^2 = furan-2yl $R^5 = C_6H_5$

	R
21, 24, 26	C_6H_5
22	C_6H_4-4Cl
23	C_6H_4-4OCH_3
25, 27	furan-2yl

Reagents and conditions: (a) RCOCl, Pyridine dry, CH_2Cl_2, reflux, 3-4 days, 20-55% yield.